

A phase-field method for propagating fluid-filled fractures coupled to a surrounding porous medium

Thomas Wick

AG Wissenschaftliches Rechnen (GWR)
Institut für Angewandte Mathematik (IfAM)

Cluster of Excellence PhoenixD
Leibniz Universität Hannover (LUH)

<https://www.ifam.uni-hannover.de/de/wick/>
<https://thomaswick.org>

May 31 - Jun 4, 2021

Interpore Conference, online

(MS24) Mathematical and computational challenges related to porous media - Special session in memory of Andro Mikelić (invitation only)

Collaborators in this work

- Mary F. Wheeler (ICES Austin, USA);
- Sanghyun Lee (Florida State University, USA);
- Andro Mikelić (Lyon, France);
- Timo Heister (Clemson, USA);
- Nima Noii (LUH, Germany);
- Fadi Aldakheel (LUH, Germany);
- Peter Wriggers (LUH, Germany)

Overview

- 1 Modeling
- 2 Phase-field fracture in elasticity
- 3 Fluid-filled phase-field fractures in poroelasticity (Andro's main contributions in this field)
 - Single-phase flow in the fracture
 - A phase-field fixed-stress algorithm
 - Numerical tests
 - Nonintrusive global-local multiscale in space
- 4 Conclusions

Phase-field / variational modeling for fracture

Key idea (Bourdin/Francfort/Marigo; 1998/2000):

- Numerical approach is based on Ambrosio-Tortorelli elliptic functionals¹;
- Discontinuities in the displacement field across the lower-dimensional crack surface \mathcal{C} are approximated by an auxiliary (smoothed indicator) function φ :

$$\Gamma_\epsilon(\varphi) = \frac{1}{2\epsilon} \|1 - \varphi\|^2 + \frac{\epsilon}{2} \|\nabla \varphi\|^2 \quad \rightarrow \quad \mathcal{H}^{d-1}(\mathcal{C}) \quad \text{for } \epsilon \rightarrow 0,$$

in the sense of the Γ -limit.

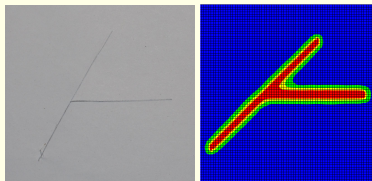


Figure: Left: Crack in a sheet of paper caused by cutting with scissors and. Right: diffusive fixed-topology finite element phase-field modeling. The transition zone (green) has width $\epsilon > h > 0$.

¹Ambrosio/Tortorelli; 1990, 1992

Modeling phase-field fracture in a nutshell

- Griffith's model for brittle fracture: **Energy functional E is minimized** with respect to kinematically admissible displacements \mathbf{u} and any crack path φ satisfying a crack growth condition

$$\partial_t \varphi \leq 0 \quad (\text{variational inequality! Rice's condition})$$

- Crack C with length l advances if energy release rate is critical:

$$\left(\frac{\partial P}{\partial l}(t, l(t)) + G_c \right) \cdot \partial_t l(t) = 0,$$

where P is the potential energy and G_c the fracture toughness.

- Variational fracture in pure elasticity: **Francfort and Marigo et al. (since 1998)**²
- Thermodynamically consistent phase-field framework: Amor et al. 2009 and Miehe et al. 2010, CMAA and IJNME
- Pressurized and fluid-filled fractures in **poroelasticity**: Mikelić et al. (since 2013, ICES report 13-15; published in 2019 in GEM)³

²Further important contributions: Bourdin, Chambolle, Dal Maso et al., Burke et al., Larsen et al., Allaire et al.

³Also other contributions from Bourdin et al. (2012), Almi et al. (2014), Miehe et al. (2015), Heider et al. (2015)

- 1 Modeling
- 2 Phase-field fracture in elasticity
- 3 Fluid-filled phase-field fractures in poroelasticity (Andro's main contributions in this field)
 - Single-phase flow in the fracture
 - A phase-field fixed-stress algorithm
 - Numerical tests
 - Nonintrusive global-local multiscale in space
- 4 Conclusions

The resulting Euler-Lagrange system

Formulation (PFF for elasticity)

Define $V := H_0^1(B)$, $W_{in} := \{w \in H^1(B) \mid w \leq \varphi^{old} \leq 1 \text{ a.e. on } B\}$, and $W := H^1(B)$. For the loading steps $n = 1, 2, 3, \dots$: Find vector-valued displacements and a scalar-valued phase-field variable $(u^n, \varphi^n) := (u, \varphi) \in \{u_D + V\} \times W$ such that

$$\left(((1 - \kappa)\varphi^2 + \kappa) \sigma(u), e(w) \right) = 0 \quad \forall w \in V, \quad (1)$$

and

$$\begin{aligned} & (1 - \kappa)(\varphi \sigma(u) : e(u), \psi - \varphi) \\ & + G_c \left(-\frac{1}{\varepsilon}(1 - \varphi, \psi - \varphi) + \varepsilon(\nabla \varphi, \nabla(\psi - \varphi)) \right) \geq 0 \quad \psi \in W_{in} \cap L^\infty(B) \end{aligned} \quad (2)$$

Therein, $\varepsilon, \kappa > 0$ and $\kappa = o(\varepsilon)$, and G_c is the critical energy release rate. Moreover,

$$\sigma := \sigma(u) = 2\mu e(u) + \lambda \operatorname{tr}(e(u))I.$$

Here, μ and λ are material parameters, $e(u) = \frac{1}{2}(\nabla u + \nabla u^T)$ is the strain tensor, and I the identity matrix. **Key challenges are:**

- Relation of ε to spatial discretization parameter h ;
- Non-convexity of the underlying energy functional due to the term

$$\left(((1 - \kappa)\varphi^2 + \kappa) \sigma(u), e(w) \right).$$

Philosophy of our analysis and discretization

- Formulation as a semi-linear form (combining both equations/inequalities for u and φ):

Formulation

For $n = 1, 2, 3, \dots$: Find $U^n := U := \{u, \varphi\} \in V \times W$ such that

$$A(U)(\Psi - U) \geq 0 \quad \forall \Psi := \{w, \psi\} \in V \times W_{in}. \quad (3)$$

- Relaxing the inequality constraint (e.g., augmented Lagrangian);
- Discretization in time (incremental formulation);
- Adaptive discretization in space;
- Newton's method (needs to be modified for fully monolithic solution!)

A monolithically-coupled formulation

Formulation

Given $\varphi^{n-1}, \tilde{\varphi} \in H^1(B)$. For the loading steps $n = 1, 2, 3, \dots$: Find $U^n := U = \{u, \varphi\} \in \{u_D + V\} \times W$ such that

$$\begin{aligned} A(U)(\Psi) &= \left(((1 - \kappa)\tilde{\varphi}^2 + \kappa) \sigma(u), e(w) \right) \\ &\quad + (1 - \kappa)(\varphi \sigma(u) : e(u), \psi) + G_c \left(-\frac{1}{\varepsilon} (1 - \varphi, \psi) + \varepsilon (\nabla \varphi, \nabla \psi) \right) \\ &\quad + ([\Xi + \gamma(\varphi - \varphi^{n-1})]^+, \psi) \\ &= 0 \quad \forall \Psi := \{w, \psi\} \in V \times W, \end{aligned}$$

where $\tilde{\varphi}$ is a linear extrapolation of φ^{n-1} and φ^{n-2} .

A monolithically-coupled formulation

Formulation

Given $\varphi^{n-1}, \tilde{\varphi} \in H^1(B)$. For the loading steps $n = 1, 2, 3, \dots$: Find $U^n := U = \{u, \varphi\} \in \{u_D + V\} \times W$ such that

$$\begin{aligned} A(U)(\Psi) &= \left(((1 - \kappa)\tilde{\varphi}^2 + \kappa) \sigma(u), e(w) \right) \\ &\quad + (1 - \kappa)(\varphi \sigma(u) : e(u), \psi) + G_c \left(-\frac{1}{\varepsilon} (1 - \varphi, \psi) + \varepsilon (\nabla \varphi, \nabla \psi) \right) \\ &\quad + ([\Xi + \gamma(\varphi - \varphi^{n-1})]^+, \psi) \\ &= 0 \quad \forall \Psi := \{w, \psi\} \in V \times W, \end{aligned}$$

where $\tilde{\varphi}$ is a linear extrapolation of φ^{n-1} and φ^{n-2} .

Why monolithic?

- 1 High accuracy of coupling conditions;
- 2 Numerical stability and implicit discretizations;
- 3 Consistent modeling of gradient-based optimization and dual-weighted error estimation;
- 4 Space-time formulations.
- 5 Finally, sometimes, the monolithic solution is even more efficient than subiterations (Gerasimov / Lorenzis; 2016, CMAME).

Adaptive spatial discretization

- Adaptive spatial discretization:
 - Galerkin finite element scheme with H^1 conforming discrete spaces $V_h \subset V$ and $W_h \subset W$ consisting of bilinear functions Q_1^c on quadrilaterals/hexahedra.
 - The **key challenge** is the relation of the model regularization parameter ε and the spatial mesh size h (high mesh resolution required!) since $h < \varepsilon$.
- **Predictor-corrector mesh adaptivity** with hanging nodes (the mesh grows with the fracture).

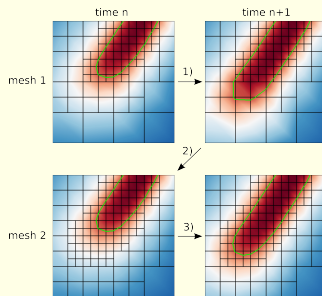
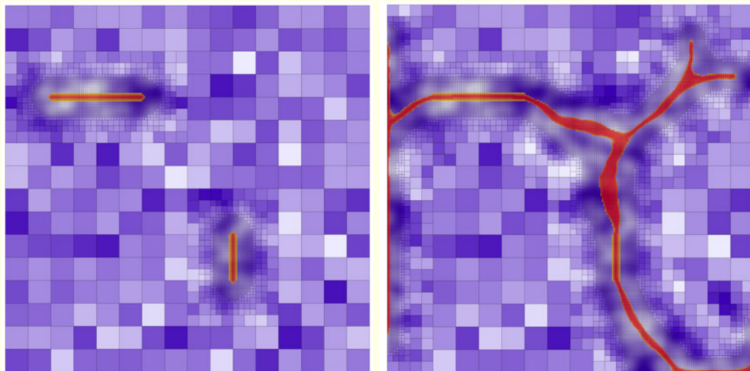


Figure: Predictor-corrector scheme: 1. advance in time, crack leaves fine mesh. 2. refine and go back in time (interpolate old solution). 3. advance in time on new mesh. Repeat until mesh doesn't change anymore. Refinement is triggered for $\varphi < C = 0.2$ (green contour line) here.

Predictor-corrector mesh refinement⁴



⁴Heister/Wheeler/Wick; CMAME, 2015

- 1 Modeling
- 2 Phase-field fracture in elasticity
- 3 Fluid-filled phase-field fractures in poroelasticity (Andro's main contributions in this field)
 - Single-phase flow in the fracture
 - A phase-field fixed-stress algorithm
 - Numerical tests
 - Nonintrusive global-local multiscale in space
- 4 Conclusions

Philosophical and practical questions

- How to model the fracture? As a 2D surface or a 3D (thin) domain?
- ⇒ Since we nevertheless work in practice with $\varepsilon > 0$, we consider the fracture as a 3D object.
- The meaning of ε ?
- ⇒ The Biot system is an upscaled model. There is an interplay between the pore size l and ε . We assume⁵ that $\varepsilon \gg l$
- How to obtain effective laws such as porosity and permeability?
- ⇒ For the permeability we work with first principle fluid equations (Navier-Stokes), derive according lubrication laws, which yield permeabilities. These are plugged into the 3D Darcy flow equations.

⁵Mikelić/Wheeler/Wick; 2015, Comp. Geosci.

Interface conditions for pressurized and fluid-filled cracks ⁶

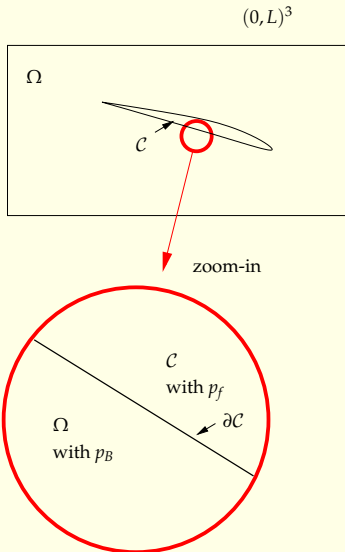
- The previous system is incomplete since force balance between \mathcal{C} and a poroelastic medium is not treated.
- Let us view \mathcal{C} as a 3D thin domain with width much less than length;
- Lubrication theory applies.
- Leading order of the stress in \mathcal{C} is $-p_f I$ and at the crack boundary we have continuity of the contact force

$$\sigma \mathbf{n} = (\mathcal{G}e(\mathbf{u}) - \alpha p_B I) \mathbf{n} = -p_f \mathbf{n}$$

$$\Rightarrow \int_{\Omega} \alpha p_B \operatorname{div} \mathbf{w} \, dx + \int_{\partial \mathcal{C}} \sigma \mathbf{n} \mathbf{w} \, dS$$

$$= \int_{\Omega} \alpha p_B \operatorname{div} \mathbf{w} \, dx - \int_{\partial \mathcal{C}} p_f w_n \, dS$$

$$= \int_{\Omega} (\alpha - 1) p_B \operatorname{div} \mathbf{w} \, dx - \int_{\Omega} \nabla p_B \mathbf{w} \, dx + \int_{\partial_N \Omega} p_B w_n \, dS$$



⁶Mikelić/Wheeler/Wick; 2019, GEM

The resulting Euler-Lagrange system

Formulation (Mikelić/Wheeler/Wick 2015 SIAM MMS)

Let $p \in H^1(B)$ be given. Find $(u, \varphi) \in \{u_D + V\} \times W$ such that

$$\begin{aligned} & \left(((1 - \kappa)\varphi_+^2 + \kappa) \sigma^+(u), e(w) \right) + (\sigma^-(u), e(w)) \\ & - (\alpha - 1)(\varphi_+^2 p, \operatorname{div} w) + (\varphi_+^2 \nabla p, w) = 0 \quad \forall w \in V, \end{aligned} \quad (4)$$

and

$$\begin{aligned} & (1 - \kappa)(\varphi \sigma^+(u) : e(u), \psi - \varphi) - 2(\alpha - 1)(\varphi_+ p \operatorname{div} u, \psi) + 2(\varphi_+ \nabla p u, \psi) \\ & + G_c \left(-\frac{1}{\varepsilon}(1 - \varphi, \psi - \varphi) + \varepsilon(\nabla \varphi, \nabla(\psi - \varphi)) \right) \geq 0 \quad \psi \in W_{in} \cap L^\infty(B), \end{aligned} \quad (5)$$

where⁷

$$\sigma^+ = 2\mu e^+ + \lambda \langle \operatorname{tr}(e) \rangle I, \quad \sigma^- = 2\mu(e - e^+) + \lambda(\operatorname{tr}(e) - \langle \operatorname{tr}(e) \rangle)I,$$

and $e^+ = P\Lambda^+P^T$, where $\langle \cdot \rangle$ is the positive part of a function. Moreover, for $d = 2$,

$$\Lambda^+ := \Lambda^+(u) := \begin{pmatrix} \langle \lambda_1(u) \rangle & 0 \\ 0 & \langle \lambda_2(u) \rangle \end{pmatrix}.$$

⁷Miehe et al. (2010); see also Amor et al. (2009) for another version

Extension to flow in porous media and the fracture ^{8 9}

A generalized pressure equation (a diffraction system):

$$\rho^0 \theta \partial_t p - \nabla \cdot \frac{K \rho^0}{\mu} (\nabla p - \rho^0 g) + \omega p = \tilde{q} \quad \text{in } \Omega,$$

where

$$\theta := \theta(x, t) := \chi_{\Omega_R} \left(\left(\frac{3\alpha^2}{3\lambda + 2\mu} + \frac{1}{M} \right) \right) + \chi_{\Omega_F} \varphi_F c_F,$$

$$\omega := \omega(x, t) := \chi_{\Omega_F} \rho_F^0 c_F \partial_t \varphi_F,$$

$$\tilde{q} := \tilde{q}(x, t) := \chi_{\Omega_R} q_R - \chi_{\Omega_R} \partial_t \left(\frac{3\alpha}{3\lambda + 2\mu} \bar{\sigma} \right) + \chi_{\Omega_F} q_F - \chi_{\Omega_F} \rho_F^0 \partial_t \varphi_F,$$

$$K := K(x, t) := \chi_{\Omega_R} K_R + \chi_{\Omega_F} K_F,$$

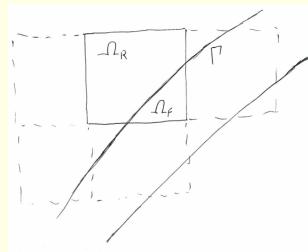
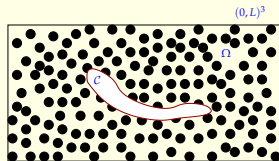
$$\mu := \mu(x, t) := \chi_{\Omega_R} \mu_R + \chi_{\Omega_F} \mu_F,$$

$$\rho^0 := \chi_{\Omega_R} \rho_R^0 + \chi_{\Omega_F} \rho_F^0.$$

The interface conditions on $\Gamma := \Omega_F \cap \Omega_R$ are given by

$$p_R = p_F,$$

$$\frac{K_R}{\mu_R} (\nabla p_R - \rho_R^0 g) \cdot n_R = \frac{w^2}{12\mu_F} (\nabla p_F - \rho_F^0 g) \cdot n_F.$$



⁸Ladyzhenskaja/Solonnikov/Uralceva; AMS Vol. 23, 1968

⁹Lions/Magenes, tome 1, chapitre 3, section 4, 1968

Three-field problem for fluid-filled fractures

- Pressure diffraction (Biot's system plus 3d lubrication): Find $p \in U := L^2(0, T; H^1(\Omega))$:

$$(\rho^0 \theta \partial_t p, \varphi^p) + \left(\frac{K \rho^0}{\mu} (\nabla p - \rho^0 g), \nabla \varphi^p \right) + (\omega p, \varphi^p) = (\tilde{q}, \varphi^p) \quad \forall \varphi^p \in U.$$

- Linear elasticity: Find $u \in V := H_0^1(\Omega)$:

$$\left(((1 - \kappa) \tilde{\varphi}^2 + \kappa) \mathcal{G}e(u), e(w) \right) - (\alpha - 1) (\tilde{\varphi}^2 p, \operatorname{div} w) + (\tilde{\varphi}^2 \nabla p, w) = 0 \quad \forall w \in V.$$

- Phase-field: Find $\varphi \in W := L^2(0, T; H^1(\Omega))$:

$$\begin{aligned} & (1 - \kappa) (\varphi \mathcal{G}e(u) : e(u), \psi) - 2(\alpha - 1) (\varphi p \operatorname{div} u, \psi) + 2 (\varphi \nabla p u, \psi) \\ & + G_c \left(-\frac{1}{\varepsilon} (1 - \varphi, \psi) + \varepsilon (\nabla \varphi, \nabla \psi) \right) \geq 0 \quad \forall \psi \in W, \end{aligned}$$

and $\partial_t \varphi \leq 0$.

- Two formulations (**monolithic** and **partially decoupled**) on the next two slides.

A monolithic form of the three-field problem¹⁰

- Convex constraint of the variational inequality assures the irreversibility and entropy compatibility of the crack formation;
- Constructing the corresponding Lyapunov functional that is linked to a generalized free energy. This procedure requires **less** regularity than a decoupled approach;
- Establishing existence of a solution to the incremental (time-discretized) problem through convergence of a finite dimensional approximation:

Theorem

There exists at least one variational solution $\{\mathbf{u}, \varphi, p\} \in V_U \times H^1(B) \cap K \times V_P$ for the variational three-field problem.

- A robust numerical solution algorithm based on Newton's method with backtracking line-search and quasi-Newton steps.

¹⁰A. Mikelić et al.; 2015, Comp. Geosci.

A decoupled form of the three-field problem via phase-field fixed-stress splitting

At each time t^n

repeat

Solve two-field fixed-stress (inner loop):

Solve the (linear) pressure diffusion problem

Solve the (nonlinear) fully-coupled elasticity phase field formulation

until Stopping criterion

$$\max\{\|p^l - p^{l-1}\|, \|u^l - u^{l-1}\|, \|\varphi^l - \varphi^{l-1}\|\} \leq \text{TOL}_{\text{FS}}, \quad \text{TOL}_{\text{FS}} > 0$$

for fixed-stress split is satisfied

Set: $(p^n, u^n, \varphi^n) := (p^l, u^l, \varphi^l)$.

Increment $t^n \rightarrow t^{n+1}$.

Remark:

For the original version of fixed stress refer to Settari/Maurits (1998) and many presentations and references given at this conference.

- 1 Modeling
- 2 Phase-field fracture in elasticity
- 3 Fluid-filled phase-field fractures in poroelasticity (Andro's main contributions in this field)
 - Single-phase flow in the fracture
 - A phase-field fixed-stress algorithm
 - Numerical tests
 - Nonintrusive global-local multiscale in space
- 4 Conclusions

Numerical Tests

Tests:

- 1 Extension to a fluid-filled Sneddon test: p is an unknown, Biot's coefficient is $\alpha = 1$ (full coupling in the poroelastic regime), phase-field fixed-stress solution algorithm;
- 2 Two parallel 3D fractures: predictor-corrector mesh adaptivity and parallel high performance computing (using p4est¹¹, trilinos¹², and MPI)

Software:

- IPACS¹³ (Integrated Phase Field Advanced Crack Simulator) based on deal.II¹⁴

¹¹<http://www.p4est.org/>

¹²<https://github.com/trilinos/Trilinos>

¹³Wheeler, Wick, Lee; CMAME, 2020

¹⁴www.dealii.org

IPACS (C++)

- Version 6.0: phase-field fracture, coupled to poroelasticity and a two-phase fluid inside the fracture¹⁵
- Approx. 16 000 lines of code, which is then based on deal.II (main coding two-phase flow April 2017 at ICES)
- 2D and 3D (switch by template parameter)
- Quadrilateral/hexahedra meshes with hanging nodes¹⁶
- Parallelized using MPI

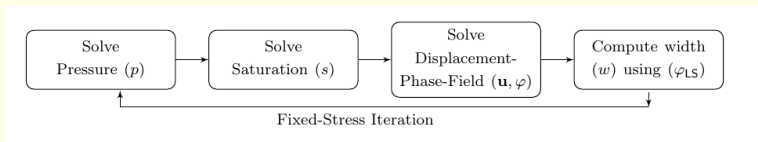
¹⁵Lee et al.; SIAM MMS, 2018; Wheeler et al. CMAME, 2020

¹⁶Carey/Oden; 1984

¹⁷Sun/Liu; SISC, 2009

IPACS (C++)

- Version 6.0: phase-field fracture, coupled to poroelasticity and a two-phase fluid inside the fracture¹⁵
- Approx. 16 000 lines of code, which is then based on deal.II (main coding two-phase flow April 2017 at ICES)
- 2D and 3D (switch by template parameter)
- Quadrilateral/hexahedra meshes with hanging nodes¹⁶
- Parallelized using MPI
- Fixed-stress / predictor-corrector mesh adaptivity solution loop:



- EG (enriched Galerkin¹⁷) for pressure and saturations (DG faces; implemented also for adaptive mesh refinement!)
- CG for displacements, phase-field, crack width

¹⁵Lee et al.; SIAM MMS, 2018; Wheeler et al. CMAME, 2020

¹⁶Carey/Oden; 1984

¹⁷Sun/Liu; SISC, 2009

Example 1

A fluid-filled fracture in poroelasticity (extension of Sneddon's test¹⁸

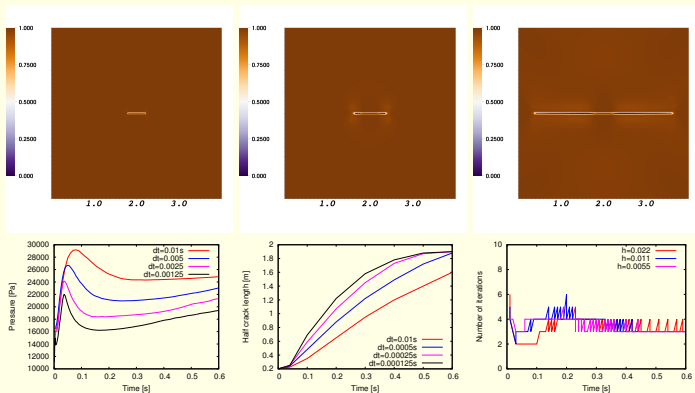


Figure: Top: fracture pattern. Bottom: temporal convergence studies of the maximum pressure, the fracture length and at right the number of fixed-stress iterations.

¹⁸Lee/Wheeler/Wick; 2017, JCAM

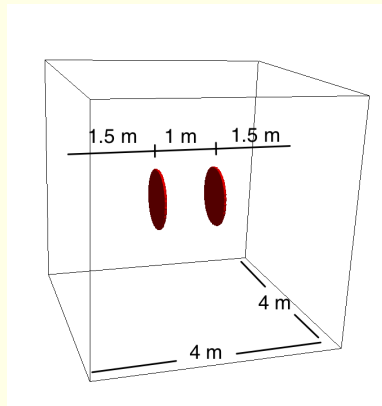
Example 2

Two parallel fractures: the setting ¹⁹

Parameters:

- Critical energy release rate:
 $G_c = 1.0 \text{ Pa} \cdot \text{m}$;
 - Lamé coefficients $\mu = 4.2 \times 10^7 \text{ Pa}$ and
 $\lambda = 2.8 \times 10^7 \text{ Pa}$;
 - Increasing pressure: $p = t \times 5 \times 10^4 \text{ Pa}$,
where t is the current time;
 - Time step size $\delta t = 0.005 \text{ s}$ and spatial
discretization parameter
 $h_{\min} = 0.0270633 \text{ m}$
- Maximum number of total DoFs is
4,074,532 (predictor-corrector
refinement);
- 17 hours total CPU time.

Configuration:



¹⁹Lee/Wheeler/Wick; 2016, CMAME

Two parallel fractures

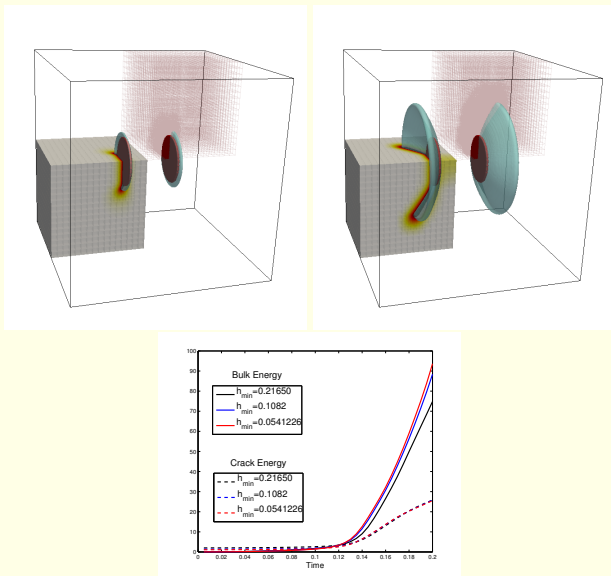
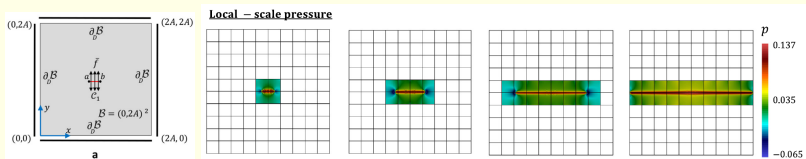


Figure: Propagation of two parallel fractures for increasing pressure for each time

- 1 Modeling
- 2 Phase-field fracture in elasticity
- 3 Fluid-filled phase-field fractures in poroelasticity (Andro's main contributions in this field)
 - Single-phase flow in the fracture
 - A phase-field fixed-stress algorithm
 - Numerical tests
 - Nonintrusive global-local multiscale in space
- 4 Conclusions

Global-local approach in porous media ²⁰

- Fluid injection into fracture inside porous medium
- Local variables: displacements u , pressure p and phase-field φ
- Global: only mechanics (displacements u)
- Predictor-corrector scheme for advancing local domain



Example1. Time and degrees of freedom comparison between the single-scale and GL problems for different reservoir sizes.

| Size of reservoir | Accumulated time, s | | | Total degrees of freedom | |
|-------------------|---------------------|----------|----------|--------------------------|--------|
| | single-scale | g/l | ratio | single-scale | g/l |
| Small | 1.9752e+04 | 849.0794 | 23.2632 | 87 723 | 18 315 |
| Medium | 6.2474e+04 | 862.3567 | 72.4453 | 171 366 | 18 665 |
| Large | 1.0559e+05 | 887.2200 | 119.0169 | 256 035 | 19 109 |

Figure: Configuration (left) and pressure evolution in the local domains (right).

- 1 Modeling
- 2 Phase-field fracture in elasticity
- 3 Fluid-filled phase-field fractures in poroelasticity (Andro's main contributions in this field)
 - Single-phase flow in the fracture
 - A phase-field fixed-stress algorithm
 - Numerical tests
 - Nonintrusive global-local multiscale in space
- 4 Conclusions

Conclusions

Conclusions

- Modeling of fluid-filled phase-field fractures in porous media
- Predictor-corrector schemes for mesh and global/local adaptivity
- Code framework (IPACS) and simulations (2D and 3D)
- Extension to a global-local multiscale approach

Conclusions

Conclusions

- Modeling of fluid-filled phase-field fractures in porous media
- Predictor-corrector schemes for mesh and global/local adaptivity
- Code framework (IPACS) and simulations (2D and 3D)
- Extension to a global-local multiscale approach

Key references of this talk

- Adaptive GL approach: N. Noii, F. Aldakheel, T. Wick, P. Wriggers; CMAME, Vol. 361 (2020), 112744
- IPACS: M.F. Wheeler, T. Wick, S. Lee; CMAME, Vol. 367 (2020), pp. 113124
- PFF fixed stress and width comp.:
S. Lee, M.F. Wheeler, T. Wick; JCAM, Vol. 314 (2017), pp. 40-60;
- Coupling PFF, poroelasticity, and single phase-fluid:
A. Mikelić, M.F. Wheeler, T. Wick; SIAM MMS, Vol. 13(1), 2015, pp. 367-398

The end

10 Meetings with Andro Mikelić have been just incredibly extraordinary, and demonstrated how mathematical PDE analysis and numerical simulations yield fruitful results. During Andro's sabbatical in the first half of 2013 at UT Austin, we had nearly every day discussions resulting in [318] and several follow-up publications. This experience has been influential to me and was an outstanding opportunity being a young Postdoc.

Figure: Quote from my book, p. IX, de Gruyter, 2020.

Thank you very much for your attention!

Thomas Wick
Institute of Applied Mathematics
Leibniz University Hannover
<https://thomaswick.org>